Advanced Optical Materials

Plasmonic nano-rotamers with programmable polarization-resolved coloration

--Manuscript Draft--

Manuscript Number:	
Article Type:	Research Article
Corresponding Author:	Hyeon-Ho Jeong, PhD GIST: Gwangju Institute of Science and Technology Gwangju, KOREA, REPUBLIC OF
Corresponding Author E-Mail:	jeong323@gist.ac.kr
Order of Authors (with Contributor Roles):	Juhwan Kim, BS (Data curation: Equal; Formal analysis: Lead; Methodology: Equal; Writing – original draft: Supporting; Writing – review & editing: Supporting)
	Jang-Hwan Han, PhD (Data curation: Equal; Formal analysis: Supporting; Methodology: Equal; Writing – original draft: Supporting; Writing – review & editing: Supporting)
	Hyun Min Kim, BS (Data curation: Supporting; Formal analysis: Supporting; Investigation: Supporting; Writing – original draft: Supporting; Writing – review & editing: Supporting)
	Tung-Chun Lee, PhD (Conceptualization: Equal; Investigation: Equal; Supervision: Equal; Validation: Equal; Visualization: Supporting; Writing – original draft: Equal; Writing – review & editing: Lead)
	Hyeon-Ho Jeong, PhD (Conceptualization: Lead; Funding acquisition: Lead; Supervision: Lead; Visualization: Lead; Writing – original draft: Lead; Writing – review & editing: Lead)
Keywords:	plasmonic rotamer; metamolecules; physical shadow growth; polarization-resolved coloration
Section/Category:	
Abstract:	We here present 3D-shaped artificial Mg nano-rotamers with a programmable dihedral angle between two plasmonic arms, designed to exhibit both programmable linear and circular polarization properties. The nanoscale physical shadow growth technique offers precise control over the angular alignment in these nanostructures with 1o angular precision, thus controlling their symmetry from achiral C2v and C2h to chiral C2. As a result, they give rise to a wide range of polarization-resolved coloration, spanning from invisible to vivid visible colors with 34% transmission contrast (for linear polarization) and 0.08 g-factor switching (for circular polarization). These nano-rotamers hold great potential for various applications in adaptive photonic filters, memory, and anticounterfeiting devices, benefiting from their tunable plasmonic properties.
Suggested Reviewers:	Ventsislav Valev, PhD Professor, University of Bath V.K.Valev@bath.ac.uk An epxert on plasmonics and spectroscopy, especially for chiral plasmonics
	Peer Fischer, PhD Professor, Max-Planck-Institute for Medical Research: Max-Planck-Institut fur medizinische Forschung peer.fischer@mr.mpg.de An expert on nanofabrication used here and chiral plasmonics
	John Gibbs, PhD Associate Professor, Northern Arizona University John.Gibbs@nau.edu An expert on nanofabrication used here and photonics
	Ambarish Ghosh, PhD Professor, Indian Institute of Science

	ambarish@iisc.ac.in An epxert on nanofabrication used here and chiral spectroscopy
	Jong Kyu Kim, PhD Professor, POSTECH: Pohang University of Science and Technology kimjk@postech.ac.kr An expert on nanofabriation used here and nanomaterials
Opposed Reviewers:	
Author Comments:	
Additional Information:	
Question	**Response**
Please submit a plain text version of your cover letter here.	Dear Editor, We herewith submit this manuscript “Plasmonic nano-rotamers with programmable polarization-resolved coloration” to be considered for publication as a Research Article in Advanced Optical Materials. We herein report the first example of plasmonic nano-rotamers made of Mg, enabling polarization-resolved coloration from invisible to visible. Inspired by an analog clock comprising two minute and hour arms, they are formed with two plasmonic nano-arms aligned with a dihedral angle. Such angular alignments are pre-programmed using the physical shadow growth method and grown in parallel at the wafer scale [Nat. Mat. 2013, 12, 807]; otherwise impossible with any other exciting methods. This unique angular engineering fidelity offers programmable polarization-resolved coloration for both linearly (34% transmission contrast) and circularly (0.08 g-factor switching) polarized lights, which we show here theoretically and experimentally. We believe this work is also of strong engineering interest due to its modulation fidelity for polarization optical effects which are for the first time programming in both linear and circular polarized light at the wafer scale. We thus see this as highly suited for the wide interdisciplinary audience of Advanced Optical Materials across nanomaterials, nanofabrication, nanophotonics, and in particular for large-scale adaptive color filters and displays. This manuscript has not been published elsewhere and has not been submitted to any other journal. All of the authors have approved the manuscript and agree with its submission to Advanced Optical Materials. Thank you for your consideration. Yours sincerely Tung-Chun Lee and Hyeon-Ho Jeong
Do you or any of your co-authors have a conflict of interest to declare?	No. The authors declare no conflict of interest.

Asst. Prof. Hyeon-Ho Jeong

School of Electrical Engineering and Computer Science
Gwangju Institute of Science and Technology
Republic of Korea
Tel. +82-62-715-2236 · e-mail. jeong323@gist.ac.kr

Editor
Advanced Optical Materials

Gwangju, 19 July 2023

Dear Editor,

We herewith submit this manuscript "**Plasmonic nano-rotamers with programmable polarization-resolved coloration**" to be considered for publication as a Research Article in *Advanced Optical Materials.*

We herein report the first example of plasmonic nano-rotamers made of Mg, enabling polarization-resolved coloration from invisible to visible. Inspired by an analog clock comprising two minute and hour arms, they are formed with two plasmonic nano-arms aligned with a dihedral angle. Such angular alignments are pre-programmed using the physical shadow growth method and grown in parallel at the wafer scale [*Nat. Mat.* **2013**, 12, 807]; otherwise impossible with any other exciting methods. This unique angular engineering fidelity offers programmable polarization-resolved coloration for both linearly (34% transmission contrast) and circularly (0.08 g-factor switching) polarized lights, which we show here theoretically and experimentally.

We believe this work is also of strong engineering interest due to its modulation fidelity for polarization optical effects which are for the first time programming in both linear and circular polarized light at the wafer scale. We thus see this as highly suited for the wide interdisciplinary audience of *Advanced Optical Materials* across nanomaterials, nanofabrication, nanophotonics, and in particular for large-scale adaptive color filters and displays.

This manuscript has not been published elsewhere and has not been submitted to any other journal. All of the authors have approved the manuscript and agree with its submission to *Advanced Optical Materials*.
Thank you for your consideration.

Yours sincerely,

Tung-Chun Lee

Associate Professor of Nanomaterials Chemistry
University College London (UCL)

Hyeon-Ho Jeong

Assistant Professor of Electrical Engineering and Computer Science
Gwangju Institute of Science and Technology

Plasmonic nano-rotamers with programmable polarization-resolved coloration

Juhwan Kim,[1,†] *Jang-Hwan Han,* [1,†] *Hyun Min Kim,*[1] *Tung-Chun Lee,*[2,3,*] *Hyeon-Ho Jeong,*[1,*]

[1] School of Electrical Engineering and Computer Science, Gwangju Institute of Science and Technology, Cheomdangwagi-ro 123, 61005 Gwangju, Republic of Korea

[2] Institute for Materials Discovery, University College London, London, WC1H 0AJ, UK

[3] Department of Chemistry, University College London, London, WC1H 0AJ, UK

(† These authors contributed equally)

* Corresponding author:
Tung-Chun Lee (tungchun.lee@ucl.ac.uk), Hyeon-Ho Jeong (jeong323@gist.ac.kr)

Keywords: plasmonic rotamer, metamolecules, physical shadow growth, polarization-resolved coloration

Abstract

We here present 3D-shaped artificial Mg nano-rotamers with a programmable dihedral angle between two plasmonic arms, designed to exhibit both programmable linear and circular polarization properties. The nanoscale physical shadow growth technique offers precise control over the angular alignment in these nanostructures with 1° angular precision, thus controlling their symmetry from achiral C_{2v} and C_{2h} to chiral C_2. As a result, they give rise to a wide range of polarization-resolved coloration, spanning from invisible to vivid visible colors with 34% transmission contrast (for linear polarization) and 0.08 g-factor switching (for circular polarization). These nano-rotamers hold great potential for various applications in adaptive photonic filters, memory, and anticounterfeiting devices, benefiting from their tunable plasmonic properties.

1. Introduction

Plasmonic molecules are discreet fundamental building blocks comprising multiple metallic nano-motifs arranged in a specific geometric form, giving rise to intriguing light-matter interactions akin to those observed in molecular systems.[1] The ability to design plasmonic molecules at the nanoscale holds immense potential for polarization-sensitive optical metamaterials that are currently beyond reach.[2–6] Plasmonic isomers, such as dimers[1] and trimers,[7] arise distinct coupled resonance when illuminated with linearly polarized light along their long axis, offering a wide range of applications in optical devices including, filters,[8,9] sensors,[10,11] and encryption.[12,13] Recent advances in nanofabrication techniques have further facilitated the realization of 3D structural nano-architecture, enabling the exploration of enantiomers, *i.e.* stereoisomers that are not superimposable with their mirror image.[14–16] Chiral helicoids[17] and helices,[18] for instance, inherently offer strong optical activity, showcasing differential plasmonic resonance when subjected to circularly polarized light. These properties find utility in molecular sensing[19] and holographic imaging devices.[20]

Expanding along this line, a fascinating molecular group to explore further is that of rotational isomers. Rotamers are molecules composed of two or more parts arranged with a specific dihedral angle, leading to unique polarization-resolved coloration in their plasmonic counterparts.[21–23] Rich programming in their associated dihedral angle allows a high degree of tunability in the symmetry ranging from achiral C_{2v} and C_{2h} to chiral C_2, potentially enabling color dynamics for both linearly and circularly polarized light in distinct spectral ranges. Recently, the DNA origami-assisted plasmonic nano-rotamers have been reported, featuring reconfigurable chiroptical responses according to the angular arrangements between the isomers.[24] This is a crucial step towards polarization-resolved plasmonic elements, but it is still hindered for large-area device applications by challenges associated with the mass production of nano-rotamers with identical optical dynamics.

Here we demonstrate a wafer-scale “lithography-free” parallel fabrication scheme to realize 3D-shaped Mg nano-rotamers acting as a dual functional plasmonic architecture, allowing us to program both linear and circular polarization-resolved coloration, which is challenging to achieve otherwise. Using a physical shadow growth technique known as glancing angle deposition (GLAD),[25,26] we demonstrate controlled precise variations in the dihedral angles of an array of nano-rotamers across from achiral C_{2v} to various types of chiral C_2 symmetric structures. This engineering flexibility results in wafer-level polarization-resolved coloration for both linearly and circularly polarized lights, spanning from transparent to vivid visible colors, opening up numerous possibilities for a wide range of nanophotonic applications.

2. Results and Discussions

2.1. Concept of plasmonic nano-rotamers

Drawing inspiration from an analog clock, which utilizes minute and hour arms to present a wide array of rotational configurations, we here present 3D-shaped nano-rotamers with controllable the dihedral angle ϕ between two arms, exhibiting polarization-resolved plasmonic resonance, **Figure 1A**. Strictly speaking, these plasmonic nano-rotamers are geometrically continuous and static, which clearly differ from those seen in their molecular counterparts.[27,28] However, their polarization-dependent plasmonic behaviors hypothetically mimic the optical characteristics of the molecular rotamers, so we believe they are still valid as 'plasmonically' acting rotamers.

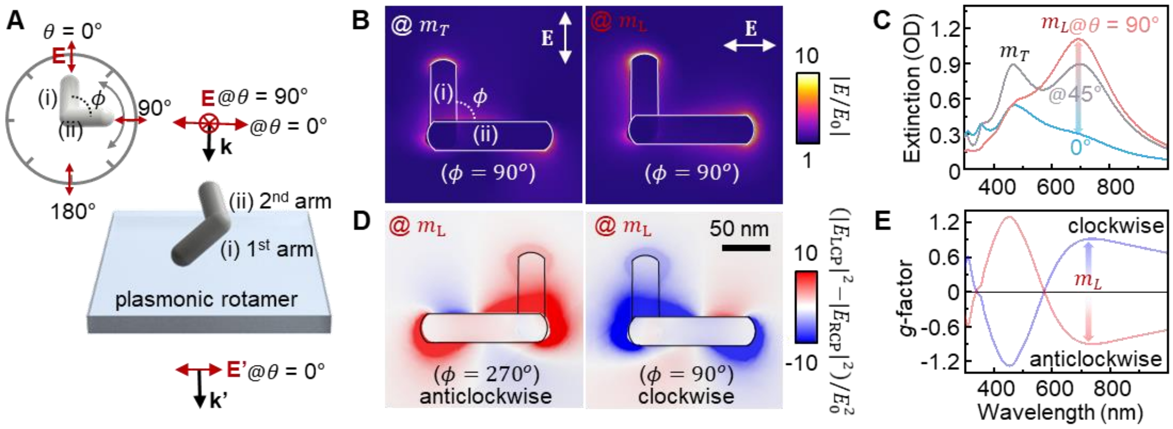

Figure 1. Plasmonic nano-rotamers with programmable polarization-resolved resonance. (a) Scheme showing a 3D-shaped plasmonic nano-rotamer with a dihedral angle $\phi = 90^o$ under two different linear polarization states ($\theta = 0^o$ and 90°) of an incident white light, where the light polarized along the 2nd arm (*i.e.* $\theta = 90^o$) is blocked by the plasmonic nano-rotamer. (b) Associated numerical calculation on optical near-field enhancement excited by a linearly polarized light at $\theta = 0^o$ for m_T mode (left) and $\theta = 90^o$ for m_L mode (right), and (c) plasmonic extinction spectra *vs.* the polarization angle θ from 0° to 90°. (d) Chiral optical near-field enhancements of the anticlockwise (left) and clockwise nano-rotamers (right) under the left and right circularly-polarized lights at resonance (e) and their g-factor.

Similar to the plasmonic characteristics of Au nanorods, which exhibit distinctive transverse (short axis, m_T) and longitudinal (long axis, m_L) resonance modes, [29] a 3D-shaped nano-rotamer, for instance, with a dihedral angle of $\phi = 90^0$ (*i.e.* c_2 symmetry) also displays two dominant features depending on the excited resonance modes, leading to different extinction spectra (Figure 1B). Notably, we employ Mg as the base material for these nano-rotamers, as it offers plasmonic resonances in the ultraviolet spectral window for small structures (*i.e.* invisible),[30] which red-shifts into the visible regime as the length increases, analogous to the tuning in resonance from the aspect ratio of the rod (Figure S1). For example, the nano-rotamer with a dihedral angle of $\phi = 90^0$ reveals distinct color (m_L mode) supported by the plasmonic extinction (*i.e.* the sum of scattering and absorption) when linearly polarized light is irradiated along its long axis of the second arm, *i.e.* $\theta = \phi = 90^0$; otherwise, the other angular components of the plasmonic nano-rotamers become transparent (m_T mode), Figure 1A. Finite element method (FEM) numerical simulations (Figure 1C) suggest that rotating the linear polarization angle in accordance with the nano-rotamer's orientation results in a vivid color change with a 40% switching contrast at m_L resonance. This is because Mg nanostructures offer resonances in UV, which remains invisible to the naked eye, while still retaining plasmonic activity (m_T) when the light polarization is misaligned with the long axis of the nano-rotamer. This property promises a switchable color appearance, transiting from invisible to vibrant colors with high spatial definition. Furthermore, the slanted structural profile of this plasmonic nano-rotamer inherently holds geometrical C_2 chirality, thus inducing discrete optical near-field enhancements when subjected to the left and right circularly polarized lights (Figure 1D). This enhancement can be further engineered with the dihedral angle ϕ and gives rise to tunable differential extinction spectra, *i.e.* coloration, Figure 1E. We experimentally confirm these phenomena using wafer-scale plasmonic nano-rotamers.

2.2. Wafer-scale array of plasmonic nano-rotamers

The large-scale parallel growth of Mg nano-rotamers using GLAD allows precise control over the size, shape, and material composition of the nanoparticles.[18][31] There are prior similar approaches, *i.e.* using GLAD-grown structures for modulating the light polarization.[32][33] They are based on a 'seed-free' conventional GLAD approach to grow irregular dielectric nanostructures with a structural resolution of several hundred nanometers. These nanostructures are able to modulate the speed (*i.e.* phase) and intensity of light when propagating through them. Meanwhile, to make the nanostructures plasmonically active, they need to be formed with metallic materials with dimensions below 100 nm, which are extremely difficult to achieve using the conventional GLAD alone. We thus introduce the nanoscale seeds to first pattern a substrate with a quasi-hexagonal array of 10 nm Au nanodots using block-copolymer micelle nanolithography (BCML), Figure S2.[34] After that, the GLAD technique is used to selectively grow slanted Mg nano-arms onto each Au nanodot through a self-shadowing effect.[35] During the growth process, due to the fast diffusion of the Mg adatoms, we introduce 5% titanium (Ti) doping, which enhances the structural shaping in 3D while preserving the strong plasmonic property.[19,36] The long axis of the arms is readily controllable within the range of 50 nm to 100 nm, as determined through analysis of the scanning electron microscopic (SEM) images *vs.* the measured thickness using the quartz crystal microbalance (QCM) monitor during growth (Figure S3). Here, to enable systematic structural engineering while emphasizing the key feature of nano-rotamers, we fix the length of the plasmonic arms to 100 nm (Figure 2A) and create nano-rotamers with varying the dihedral angle ϕ by simply rotating the azimuthal angle of the substrate matching to ϕ and growing identical slanted 2nd Mg arms on top, *e.g.* Figure 2E and Figure S4. In contrast to their classical molecular analogs, *e.g.* *n*-butane and H_2O_2 at room temperature,[37,38] these GLAD-grown nano-rotamers are structurally static at room temperature due to the high rotational kinetic barrier at the connection between the two arms compared to thermal energy, and thus cannot interconvert. They nevertheless exhibit much stronger polarization-resolved coloration compared to the angular polarizability of molecular rotamers, which is indeed beneficial for device application.

The optical characteristics of the GLAD-grown plasmonic single nano-arms and nano-rotamers (double arms with a dihedral angle) are examined and imaged under white light source with a linear polarizer (polarization angular rotation from 0^{o} to 180^{o} with 5^{o} intervals), **Figure 2**. A monolayer of single Mg plasmonic arms give rise to the plasmonic extinction of approximately 0.2 optical density, OD (82% decay in transmittance) at m_L in visible (601 nm of wavelength) when linearly polarized light is irradiated along the long axis of the nanostructure at $\theta = 0^o$. This plasmonic extinction diminishes completely down to 0.02 OD when the polarization axis turns to $\theta = 90^o$ (*i.e.* normal to the long axis of the single arms), Figure 2C,D. Crucially the plasmonic nano-rotamers with $\phi = 0^o$ (Figure 2E) display nearly identical spectral features but exhibit twice larger switching contrast compared to the single arms, Figure 2F,G. This enhancement in the contrast arises from the fact that the number of plasmonic resonators is double in the optical path (Figure S5), suggesting that even larger switching contrast can be achieved by increasing the number of arms *viz.* zigzag structures. Note that, due to inherent challenges involved in parallel growth at the nanoscale, including (i) imperfections in the array of Au nanodots for the GLAD process, (ii) fluctuations in the deposition rate due to the low melting temperature of Mg, and (iii) high diffusion of Mg adatoms on the surface, there is a considerable variation in size and shape among the nano-rotamers, leading to broadened harmonic resonance spectra. Nonetheless, such broad resonance spectra across the whole visible range by averaging optical responses of a large number of nano-rotamers within the beam spot area of 0.8 cm^2 indeed hold potential for various photonic device applications including photodetectors and photovoltaics.[39–41] More crucially, these spectra still function to fully switch off through the whole visible spectra at $\theta = 90^o$. We, therefore, observe almost identical optical dynamics under the same polarization conditions for both single nano-arms and nano-rotamers across the entire visible spectra (Figure 2H), establishing a crucial basis for exploring various types of nano-rotamers with dihedral angular engineering.

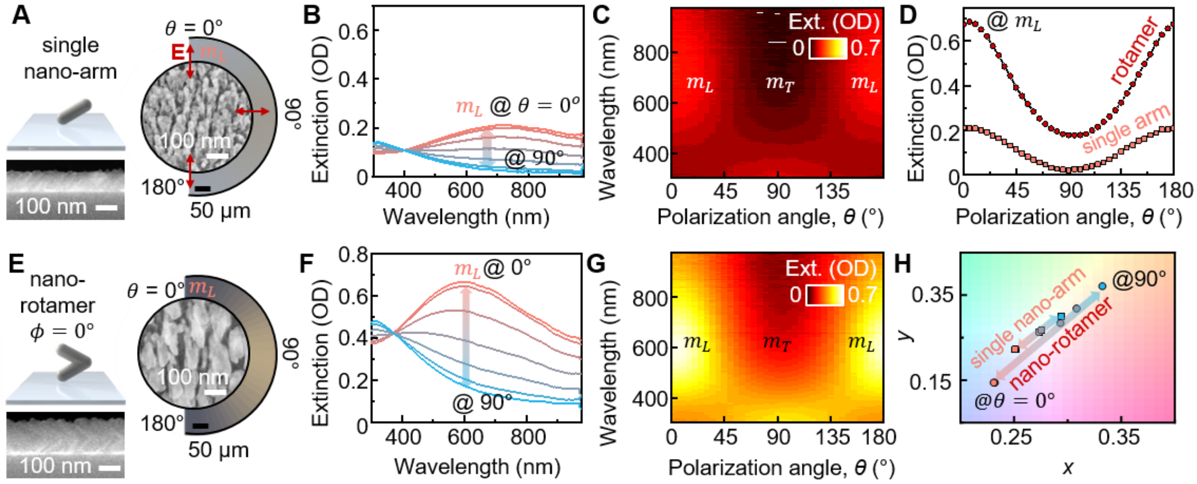

Figure 2. Plasmonic single nano-arms and nano-rotamers with double arms for C_{2v} symmetry. (a) An array of plasmonic single nano-arms (half-circular inset: their transmitted coloration) and (b) their extinction spectra, (c) linear polarization-resolved extinction in the 2D map, and (d) peak intensities *vs.* the polarization angle, θ ranging from 0° to 180°. (e) An array of plasmonic nano-rotamers with a dihedral angle, $\phi = 0^o$ (half-circular inset: their transmitted coloration) and (f) their extinction spectra, (g) linear polarization-resolved extinction in 2D map *vs.* the polarization angle, θ. (h) 1913 CIE plot of the transmitted colors through the plasmonic single nano-arms and nano-rotamers with $\phi = 0^o$.

2.3. Plasmonic nano-rotamers with angular rotation engineering

To investigate how this nano-rotamer's optical dynamics are sensitive to structural parameters, we fabricate a series of the plasmonic nano-rotamers with various dihedral angles $\phi = 45^o, 90^o, 135^o$(**Figure 3**), verified through SEM imaging (Figure 3A). Since these plasmonic nano-rotamers possess C_2 chiral symmetry, they thus differently response to linearly as well as circularly polarized lights. Firstly, we analyze their optical dynamics in response to the linearly polarized white light with the angular rotation from 0° to 180° with 5° intervals, Figure 3B. The spectral tuning of the nano-rotamers as a function of the dihedral angle ϕ is characterized experimentally and compared to simulation results, revealing a characteristic reversible 30% switching contrast (Figure 3C). Notably, almost identical color spectra across the whole visible range arise when the light polarization is aligned with every two long axes of the rotamers, unless otherwise remaining centred around in the CIE plot indicating invisible (Figure 3D).

These excellent dynamic optical performance, coupled with high fidelity in angular engineering, are found to be in reasonable agreement with the predictions of the numerical simulation (Figure S6,7). The polarization-resolved coloration, featuring a transition from color to transparency, presents exciting opportunities for modulating light transmission in various photonic applications including adaptive color filters,[22,42,43] optical memory and security devices,[44,45] and covert display.[33]

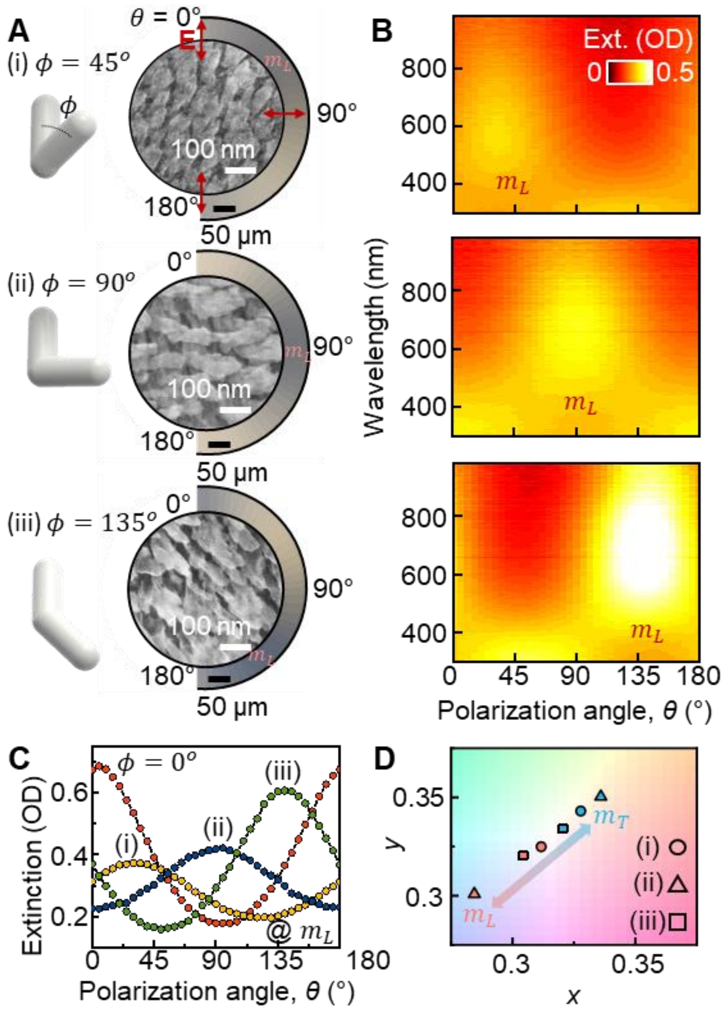

Figure 3. Plasmonic nano-rotamers with varying dihedral angles. (a) An array of plasmonic nano-rotamers with dihedral angles, $\phi = 45^o, 90^o, 135^o$ (from top to bottom, each half-circular inset: their transmitted coloration). (b) their associated 2D maps of extinction spectra, (c) peak intensities, and (d) CIE plots as a function of the polarization angle, θ ranging from 0° to 180°.

We stress that thanks to the slanted structural profiles of these plasmonic nano-rotamers with intrinsic geometrical C_2 chirality, strong chiroptical responses with significant spectral switching are possible in the visible range when illuminated with circularly polarized white lights, **Figure 4**. The circular dichroism (CD) spectra provide a means to identify the chiroptical properties of the plasmonic nano-rotamers by differentiating their extinction in response to the left and right circularly polarized lights, Figure 4A. Remarkably, the plasmonic nano-rotamers with clockwise rotation angles of $\phi = 0^o,\ 45^o, 90^o, 135^o$ exhibit consistent polar CD spectra with large g-factor tuning from near 0 to 0.08 (Figure 4B) which can be reversed when the rotation is anticlockwise.[24] These experimental findings are in excellent agreement with the numerically simulated spectra, where the associated chiroptical near-field enhancements vary with the rotational angle, thus causing the observed tuning of the CD spectra (Figure 4C). Indeed, further tuning in the CD spectra might be possible by engineering the angular rotation of the plasmonic nano-rotamers or by repeating the arms with complex arrangements. We believe that such fine tunability in the chiroptical response of the plasmonic nano-rotamers holds great promise for chirality-driven photonic applications including chiral sensing[46–48] add and holographic imaging,[20] enantiomeric separation,[49,50] and chiral-sensitive photo-synthesis[51] and photo-catalysts.[52,53] Furthermore, although we here deliberately limit the geometrical and material parameters of the plasmonic nano-rotamers to solely highlight the angular engineering fidelity for extensive switching in both linear and circular light polarizations, exploring further engineering spaces may potentially enable rich polarization-resolved coloration, *e.g.* geometry (length and angle), materials, and number of arms of the rotamer.

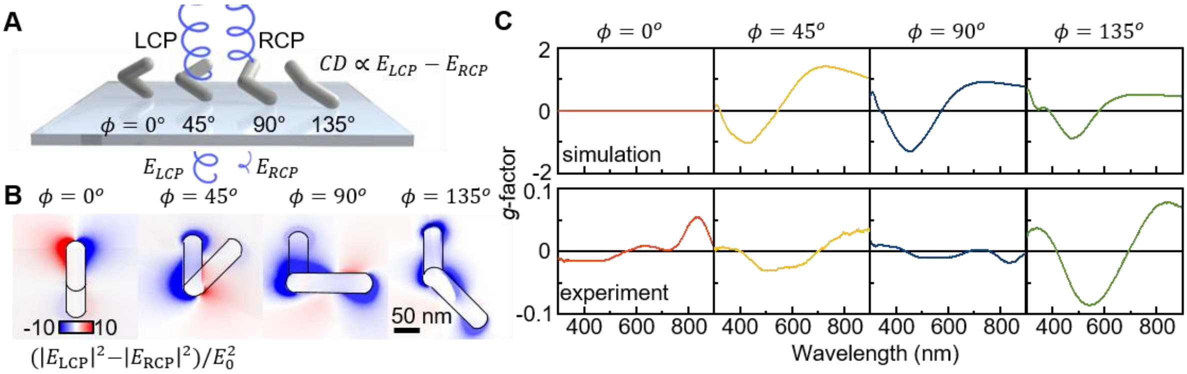

Figure 4. Plasmonic nano-rotamers with chiroptical response. (a) Scheme showing a plasmonic nano-rotamers under two different circular polarization states of an incident white light. (b) Chiroptical near-field enhancement of the nano-rotamers with dihedral angles, $\phi = 0^o, 45^o, 90^o,\ 135^o$. (c) Associated experimentally measured (top panel) and numerically calculated (bottom panel) plasmonic extinction spectra.

3. Conclusion

In conclusion, we successfully demonstrate the clock-inspired design of 3D-shaped artificial nano-rotamers made of Mg and their fabrication and optical characterization at the wafer-scale, enabling dual programming in linear and circular polarization-resolved colorations. Through the utilization of a physical shadow growth technique, we achieve precise control over the geometrical angular alignment of the plasmonic nano-rotamers, *i.e.* dihedral angular engineering. This engineering fidelity leads to polarization-resolved reversible coloration switching from invisible to vivid visible colors with 34% contrast (for linear polarization) and 0.08% g-factor tuning (for circular polarization) through the entire visible range. Such unique optical properties of these plasmonic nano-rotamers, combined with their "lithography-free" parallel fabrication scheme allows for scalability and large-scale production, paving the way for practical implementation in various polarization-resolved photonic device applications.

4. Experimental Section

Numerical Simulation: Finite element method using commercial software (COMSOL wave optics module) is used to simulate the optical response of the Mg plasmonic structures on the quartz substrate, assumed to be constant $n = 1.45$ for calculation simplicity. Periodic boundary conditions are infinitely set along x- and y-axes while the perfectly matched layer is formed on both sides of z-axis. Optical properties of Mg are taken from the literature.[54]

Block Copolymer Micelle Nanolithography: 10 nm Au nanodots are patterned on the substrate using block copolymer micelle nanolithography (BCML) as previously reported.[55] The block-copolymer micelles of poly(styrene)-b-poly(2-vinyl pyridine) self-assemble in toluene, encapsulating Au salts in their cores. These micelles are then spin-coated onto the 2-inch silicon wafer (for imaging analysis) and quartz substrate (for optical measurement), resulting in a quasi-hexagonal ordered monolayer with a spacing of approximately 100 nm. To remove the polymers and reduce the Au salts, we subject the sample to a 9:1 gas mixture of an Ar and an O_2 plasma process (100 W, 140 min, 5×10^{-3} torr). This transforms the micelles into Au nanodots with an average diameter of 10 nm, acting as seeds for subsequent GLAD growth.

Glancing angle deposition: GLAD is used to selectively grow slanted Mg nano-arms onto each Au nanodot through a self-shadowing effect. The growth is carried out at an angle of $\alpha = 85°$ and temperature of about 238 K in a vacuum chamber with a base pressure of 4×10^{-6} Torr. During the growth, Mg and Ti are co-deposited with rates of 0.1 nm/s for Mg and 0.004 nm/s for Ti. After the growth of Mg single nano-arms, the second growth of the nano-arms is carried out after azimuthally rotating the sample holder to the desired dihedral angle, including $\phi = 0°$, 45°, 90°, and 135°.

SEM analysis: SEM images of the Mg nano-arms and rotamers are obtained using a Verios 5 UC SEM (Thermo Fisher Scientific) at an accelerating voltage of 10 kV.

Optical characterization: Transmitted color images of fabricated samples are taken with a CCD camera (STC-MCS500U3V, Sentech) through 20× objective (Olympus MPLFLN-BD) in an inverted optical microscope (Olympus GX53) integrated with a linear polarizer (Broadband Polarizer, Edmund Optics) covering a wavelength range from 300 nm to 2700 nm (polarization angular rotation from 0^o to 180^o with 5^o intervals). The optical extinction spectra are measured with a fiber-optic spectroscopic system (DH-mini deuterium halogen light source, QE Pro spectrometer, Ocean Optics) with the same linear polarizer. A quarter waveplate (Achromatic waveplate, Edmund Optics) is additionally inserted in the optical path after the linear polarizer to generate left and right circularly polarized light for measurement of chiroptical properties.

Supporting Information

Supporting Information is available from the Wiley Online Library or from the author.

Acknowledgments

We are grateful to the NanoSystems Laboratory at GIST for technical support. We also thank to the GIST Central Research Facilities (GCRF) for technical assistance with the SEM imaging and the GIST Nanoinfra for Compound Semiconductors (G-NICS) for access to the cleanroom. This work was supported by the National Research Foundation of Korea (NRF) grant funded by the Korean government (MSIT) (No. NRF-2021R1C1C1005060, NRF-2021M3H3A1037899) and 'regional innovation mega project' program through the Korea Innovation Foundation (2023-DD-UP-0015). J.-H.H. acknowledges support from the AI-based GIST Research Scientist Project.

Received: ((will be filled in by the editorial staff))
Revised: ((will be filled in by the editorial staff))
Published online: ((will be filled in by the editorial staff))

References

[1] H.-H. Jeong, M. C. Adams, J.-P. Günther, M. Alarcón-Correa, I. Kim, E. Choi, C. Miksch, A. F. Mark, A. G. Mark, P. Fischer, *ACS Nano* **2019**, *13*, 11453–11459.

[2] G. Haran, L. Chuntonov, *Chem. Rev.* **2018**, *118*, 5539–5580.

[3] N. Zohar, L. Chuntonov, G. Haran, *J. Photochem. Photobiol. C Photochem. Rev.* **2014**, *21*, 26–39.

[4] R. E. Armstrong, M. Horáček, P. Zijlstra, *Small* **2020**, *16*, 2003934.

[5] A. N. Koya, *Adv. Photonics Res.* **2022**, *3*, 2100325.

[6] J.-H. Han, D. Kim, J. Kim, G. Kim, J. T. Kim, H.-H. Jeong, *Nanophotonics* **2022**, DOI doi:10.1515/nanoph-2021-0806.

[7] G. Davison, T. Jones, J. Liu, J. Kim, Y. Yin, D. Kim, W.-I. K. Chio, I. P. Parkin, H.-H. Jeong, T.-C. Lee, *Adv. Mater. Technol.* **2023**, *8*, 2201400.

[8] T. Shegai, S. Chen, V. D. Miljković, G. Zengin, P. Johansson, M. Käll, *Nat. Commun.* **2011**, *2*, 481.

[9] T. Ellenbogen, K. Seo, K. B. Crozier, *Nano Lett.* **2012**, *12*, 1026–1031.

[10] L. Chuntonov, G. Haran, *Nano Lett.* **2013**, *13*, 1285–1290.

[11] D. Punj, R. Regmi, A. Devilez, R. Plauchu, S. B. Moparthi, B. Stout, N. Bonod, H. Rigneault, J. Wenger, *ACS Photonics* **2015**, *2*, 1099–1107.

[12] P. Zheng, Q. Dai, Z. Li, Z. Ye, J. Xiong, H.-C. Liu, G. Zheng, S. Zhang, *Sci. Adv.* **2023**, *7*, eabg0363.

[13] M. Song, D. Wang, Z. A. Kudyshev, Y. Xuan, Z. Wang, A. Boltasseva, V. M. Shalaev, A. V Kildishev, *Laser Photon. Rev.* **2021**, *15*, 2000343.

[14] M. Hentschel, M. Schäferling, X. Duan, H. Giessen, N. Liu, *Sci. Adv.* **2023**, *3*, e1602735.

[15] J. T. Collins, C. Kuppe, D. C. Hooper, C. Sibilia, M. Centini, V. K. Valev, *Adv. Opt. Mater.* **2017**, *5*, 1700182.

[16] E. S. A. Goerlitzer, A. S. Puri, J. J. Moses, L. V Poulikakos, N. Vogel, *Adv. Opt. Mater.* **2021**, *9*, 2100378.

[17] H.-E. Lee, H.-Y. Ahn, J. Mun, Y. Y. Lee, M. Kim, N. H. Cho, K. Chang, W. S. Kim, J. Rho, K. T. Nam, *Nature* **2018**, *556*, 360–365.

[18] A. G. Mark, J. G. Gibbs, T.-C. Lee, P. Fischer, *Nat. Mater.* **2013**, *12*, 802–807.

[19] H.-H. Jeong, A. G. Mark, M. Alarcón-Correa, I. Kim, P. Oswald, T.-C. Lee, P. Fischer, *Nat. Commun.* **2016**, *7*, 11331.

[20] M. Khorasaninejad, A. Ambrosio, P. Kanhaiya, F. Capasso, *Sci. Adv.* **2023**, *2*, e1501258.

[21] M. Sharma, N. Hendler, T. Ellenbogen, *Adv. Opt. Mater.* **2020**, *8*, 1901182.

[22] E. Heydari, J. R. Sperling, S. L. Neale, A. W. Clark, *Adv. Funct. Mater.* **2017**, *27*, 1701866.

[23] Z. Li, A. W. Clark, J. M. Cooper, *ACS Nano* **2016**, *10*, 492–498.

[24] L. Xin, C. Zhou, X. Duan, N. Liu, *Nat. Commun.* **2019**, *10*, 5394.

[25] J.-H. Han, D. Kim, J. Kim, G. Kim, P. Fischer, H.-H. Jeong, *Adv. Mater.* **2022**, *n/a*, 2107917.

[26] K. Robbie, M. J. Brett, A. Lakhtakia, *Nature* **1996**, *384*, 616.

[27] Y. Zhang, C. Yu, T. Shan, Y. Chen, Y. Wang, M. Xie, T. Li, Z. Yang, H. Zhong, *Cell Reports Phys. Sci.* **2022**, *3*, 100765.

[28] M. Sharafi, J. P. Campbell, S. C. Rajappan, N. Dudkina, D. L. Gray, T. J. Woods, J. Li, S. T. Schneebeli, *Angew. Chemie Int. Ed.* **2017**, *56*, 7097–7101.

[29] Y. Fang, W.-S. Chang, B. Willingham, P. Swanglap, S. Dominguez-Medina, S. Link, *ACS Nano* **2012**, *6*, 7177–7184.

[30] H.-H. Jeong, A. G. Mark, P. Fischer, *Chem. Commun.* **2016**, *52*, 12179–12182.

[31] J. G. Gibbs, A. G. Mark, T.-C. Lee, S. Eslami, D. Schamel, P. Fischer, *Nanoscale* **2014**, *6*, 9457–9466.

[32] S. Larson, H. Luong, C. Song, Y. Zhao, *J. Phys. Chem. C* **2019**, *123*, 5634–5641.

[33] J. H. Ko, Y. J. Yoo, Y. J. Kim, S.-S. Lee, Y. M. Song, *Adv. Funct. Mater.* **2020**, *30*, 1908592.

[34] Roman Glass, Martin Möller, Joachim P Spatz, *Nanotechnology* **2003**, *14*, 1153.

[35] H.-H. Jeong, M. Alarcón-Correa, A. G. Mark, K. Son, T.-C. Lee, P. Fischer, *Adv. Sci.* **2017**, *4*, 1700234.

[36] Y. He, G. Larsen, X. Li, W. Ingram, F. Chen, Y. Zhao, *Adv. Opt. Mater.* **2015**, *3*, 342–346.

[37] Y. Mo, *J. Org. Chem.* **2010**, *75*, 2733–2736.

[38] Y. Mo, *WIREs Comput. Mol. Sci.* **2011**, *1*, 164–171.

[39] B. Y. Zheng, Y. Wang, P. Nordlander, N. J. Halas, *Adv. Mater.* **2014**, *26*, 6318–6323.

[40] R. A. Pala, J. White, E. Barnard, J. Liu, M. L. Brongersma, *Adv. Mater.* **2009**, *21*, 3504–3509.

[41] S. D. Namgung, R. M. Kim, Y.-C. Lim, J. W. Lee, N. H. Cho, H. Kim, J.-S. Huh, H. Rhee, S. Nah, M.-K. Song, J.-Y. Kwon, K. T. Nam, *Nat. Commun.* **2022**, *13*, 5081.

[42] H. Jia, Q. J. Wu, C. Jiang, H. Wang, L. Q. Wang, J. Z. Jiang, D. X. Zhang, *Appl. Opt.* **2019**, *58*, 704–711.

[43] Y. Jung, H. Jung, H. Choi, H. Lee, *Nano Lett.* **2020**, *20*, 6344–6350.

[44] R. Feng, H. Wang, Y. Cao, Y. Zhang, R. J. H. Ng, Y. S. Tan, F. Sun, C.-W. Qiu, J. K. W. Yang, W. Ding, *Adv. Funct. Mater.* **2022**, *32*, 2108437.

[45] Y. Chen, X. Yang, J. Gao, *Light Sci. Appl.* **2019**, *8*, 45.

[46] R. M. Kim, J.-H. Huh, S. Yoo, T. G. Kim, C. Kim, H. Kim, J. H. Han, N. H. Cho, Y.-C. Lim, S. W. Im, E. Im, J. R. Jeong, M. H. Lee, T.-Y. Yoon, H.-Y. Lee, Q.-H. Park, S. Lee, K. T. Nam, *Nature* **2022**, *612*, 470–476.

[47] J. T. Collins, K. R. Rusimova, D. C. Hooper, H.-H. Jeong, L. Ohnoutek, F. Pradaux-Caggiano, T. Verbiest, D. R. Carbery, P. Fischer, V. K. Valev, *Phys. Rev. X* **2019**, *9*, 11024.

[48] L. Ohnoutek, H.-H. Jeong, R. R. Jones, J. Sachs, B. J. Olohan, D.-M. Răsădean, G. D. Pantoş, D. L. Andrews, P. Fischer, V. K. Valev, *Laser Photon. Rev.* **2021**, *15*, 2100235.

[49] Y. Zhao, A. A. E. Saleh, J. A. Dionne, *ACS Photonics* **2016**, *3*, 304–309.

[50] J. García-Guirado, M. Svedendahl, J. Puigdollers, R. Quidant, *Nano Lett.* **2018**, *18*, 6279–6285.

[51] X. Lu, X. Wang, S. Wang, T. Ding, *Nat. Commun.* **2023**, *14*, 1422.

[52] L. Tan, S.-J. Yu, Y. Jin, J. Li, P. Wang, *Angew. Chemie Int. Ed.* **2022**, *61*, e202112400.

[53] Y. Negrín-Montecelo, A. Movsesyan, J. Gao, S. Burger, Z. M. Wang, S. Nlate, E. Pouget, R. Oda, M. Comesaña-Hermo, A. O. Govorov, M. A. Correa-Duarte, *J. Am. Chem. Soc.* **2022**, *144*, 1663–1671.

[54] K. J. Palm, J. B. Murray, T. C. Narayan, J. N. Munday, *ACS Photonics* **2018**, *5*, 4677–4686.

[55] R. Glass, M. M ller, J. P. Spatz, *Nanotechnology* **2003**, *14*, 1153–1160.

TOC

Plasmonic nano-rotamers with programmable polarization-resolved coloration

Juhwan Kim,[1,†] *Jang-Hwan Han,* [1,†] *Hyun Min Kim,*[1] *Tung-Chun Lee,*[2,3,*] *Hyeon-Ho Jeong,*[1,*]

Keywords: plasmonic rotamer, metamolecules, physical shadow growth, polarization-resolved coloration

The physical shadow growth at the nanoscale offers a wafer-scale array of 3D-shaped artificial Mg nano-rotamers with a programmable dihedral angle between two plasmonic arms. They are designed to exhibit programmable both linear and circular polarization-resolved colorations, spanning from invisible to visible colors, potentially useful for various applications in nanophotonic devices.